Dalton Transactions

PAPER

View Article Online
View Journal | View Issue

Open Access Article. Published on 09 November 2015. Downloaded on 1/25/2026 11:42:48 AM.
This article is licensed under a Creative Commons Attribution 3.0 Unported Licence.

Cite this: *Dalton Trans.*, 2015, **44**, 20514

Activation of molecular oxygen by a molybdenum complex for catalytic oxidation†

Antoine Dupé,‡[a] Martina E. Judmaier,‡[a] Ferdinand Belaj,[a] Klaus Zangger[b] and Nadia C. Mösch-Zanetti*[a]

Received 30th July 2015,
Accepted 30th October 2015

DOI: 10.1039/c5dt02931g

www.rsc.org/dalton

A sterically demanding molybdenum(VI) dioxo complex was found to catalytically activate molecular oxygen and to transfer its oxygen atoms to phosphines. Intermediate peroxo as well as reduced mono-oxo complexes were isolated and fully characterized. Monomeric Mo(IV) monooxo species proved to be of an unusual nature with the coordinated phosphine *trans* to the oxo group. The reduced molybdenum centers can activate O_2 to form a stable Mo(VI) oxo–peroxo complex unambiguously characterized by single crystal X-ray diffraction analysis. NMR experiments demonstrate that both oxygen atoms of the peroxo unit are transferred to an accepting substrate, generating the Mo(IV) intermediate and restarting the catalytic cycle.

Introduction

High-valent molybdenum-oxo complexes are of considerable interest as catalysts for oxidation reactions.[1,2] In nature, molybdenum oxotransferases are a broad class of enzymes that transfer an oxygen atom to or from a substrate, using mainly water as a source of oxygen.[3] The active site of these enzymes consists of a molybdenum(VI) center substituted by at least one oxo group and one or two molybdopterin ligands.[4] In order to mimic the activity of such enzymes, a wide range of model compounds containing a high valent $[MoO_2]^{2+}$ core have been prepared.[5] While oxygen atom transfer (OAT) capability of such complexes can be investigated using phosphines or sulfides as oxygen accepting substrates, they are also commonly used as catalysts for alkene epoxidation reactions and have thus found wide applications in industry.[6] In the most efficient systems, *tert*-butyl hydroperoxide or hydrogen peroxide solutions are used as oxidant.[1,7] However, following the principles of sustainable chemistry, the use of molecular oxygen as oxidant would be highly desirable; it is abundant, cheap, readily available and ideally does not lead to the formation of side-products.[8] Despite these advantages, controlling the reactivity of dioxygen with transition metal centers is a challenge. Although many iron, manganese and copper complexes are known to react with dioxygen,[9] only rare examples of molecular oxygen activation by molybdenum have been previously reported,[10,11] including one by our group,[12] and the reactivity of these oxo–peroxo molybdenum is limited. Few homogeneously molybdenum catalyzed oxidations employing molecular oxygen were reported. A bimetallic molybdenum/copper catalyst was disclosed by Osborn and coworkers for the oxidation of alcohols.[13] It represents a "Wacker-type reaction" where the alcohol is oxidized by molybdenum but reoxidation is mediated by the copper co-catalyst and not by molecular oxygen directly. Selected reports can be found in literature where O_2 was used in Mo catalyzed oxidation chemistry[14] but high catalyst loadings were needed and/or it remains unclear whether autooxidation is occurring.

In the course of our ongoing research on high-valent molybdenum-oxo complexes bearing Schiff-base ligands and their reactivity in OAT reactions,[15–17] we report herein the synthesis and characterization of a new molybdenum(VI) dioxo complex which can be reduced and subsequently activate dioxygen to form a new molybdenum(VI) oxo–peroxo complex. This activation proceeds *via* the formation of a five-coordinated molybdenum(IV) mono-oxo complex or a highly unusual *trans*-$[MoO(PMe)_3]^{2+}$ intermediate which was characterized by NMR spectroscopy and elemental analysis. Furthermore, we demonstrate that the molybdenum(VI) oxo–peroxo complex is also active in OAT reaction and able to transfer both oxygen atoms of the peroxo moiety to an accepting substrate. Benchmark oxidation of tertiary phosphine[18] confirms the catalytic activity of the complexes. This reactivity is a new step toward the use of oxygen as oxidant in molybdenum-catalyzed oxidation reactions.

[a]*Institute of Chemistry, University of Graz, Schubertstrasse 1, 8010 Graz, Austria. E-mail: nadia.moesch@uni-graz.at*
[b]*Institute of Chemistry, University of Graz, Heinrichstraße 28/II, 8010 Graz, Austria*
†Electronic supplementary information (ESI) available: Experimental procedures, X-ray crystallographic data, characterization data. CCDC 1413968 for **1** and 1413969 for **4**. For ESI and crystallographic data in CIF or other electronic format see DOI: 10.1039/c5dt02931g
‡These authors contributed equally to this work.

This journal is © The Royal Society of Chemistry 2015

Open Access Article. Published on 09 November 2015. Downloaded on 1/25/2026 11:42:48 AM.
This article is licensed under a Creative Commons Attribution 3.0 Unported Licence.

Results and discussion

The molybdenum-dioxo complex $[MoO_2L_2]$ **1** was synthesized by addition of a solution of the ligand 2,4-di-*tert*-butyl-6-((*tert*-butylimino)methyl)phenol (HL)[19] in toluene to a solution of 1 equiv. of $[MoO_2Cl_2]$ in toluene in presence of an excess trimethylamine (Scheme 1). After stirring for 15 h, filtration and washing with cold pentane, **1** was obtained as a orange solid in good yield (64%). The ^{1}H NMR spectrum reveals the formation of a single, symmetric isomer as only one set of resonances for both coordinated ligands is observed. The IR spectrum of **1** exhibits two strong $\nu_{Mo=O}$ bands at 885 and 912 cm^{-1} for both the symmetric and asymmetric stretching mode of the *cis*-$[MoO_2]^{2+}$ fragment, in good accordance with the literature.[16,20] Mass spectrometry as well as elemental analysis confirmed the formation of complex **1** as $[MoO_2L_2]$.

This structure was confirmed by single crystal X-ray diffraction analysis. Suitable crystals were obtained from concentrated solution of **1** in toluene (Fig. 1). Crystal data and structure refinements are presented in the Experimental section. Complex **1** exhibits a six-coordinate metal center in a distorted octahedral geometry.

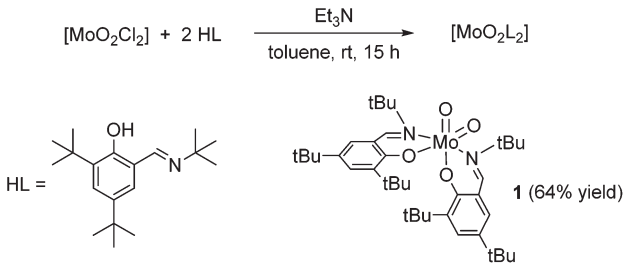

Scheme 1 Synthesis of Mo–dioxo complex **1**.

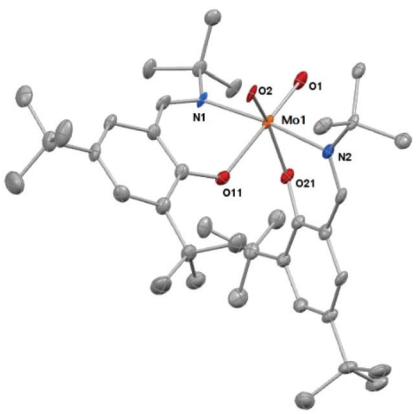

Fig. 1 Molecular structure of complex **1**. Thermal ellipsoids have been drawn at 50% probability level. Hydrogen atoms are omitted for clarity. Selected bonds lengths (Å) and angles (°): Mo(1)–O(2) 1.709(3); Mo(1)–O(1) 1.720(3); Mo(1)–O(21) 2.037(3); Mo(1)–O(11) 2.105(3); Mo(1)–N(1) 2.187(3); Mo(1)–N(2) 2.228(4); O(11)–C(11) 1.309(5); C(1)–N(1) 1.290(6); N(1)–C(10) 1.518(5); O(21)–C(21) 1.345(5); C(2)–N(2) 1.311(5); N(2)–C(20) 1.528(6); N(1)–Mo(1)–N(2) 171.91(13); O(1)–Mo(1)–O(11) 165.89(13); O(2)–Mo(1)–O(21) 159.04(13); C(11)–O(11)–Mo(1) 124.1(3); C(1)–N(1)–C(10) 116.0(3); C(1)–N(1)–Mo(1) 116.9(3); C(10)–N(1)–Mo(1) 124.8(3); C(21)–O(21)–Mo(1) 131.2(3); C(2)–N(2)–C(20) 116.0(3); C(2)–N(2)–Mo(1) 121.8(3); C(20)–N(2)–Mo(1) 121.7(3).

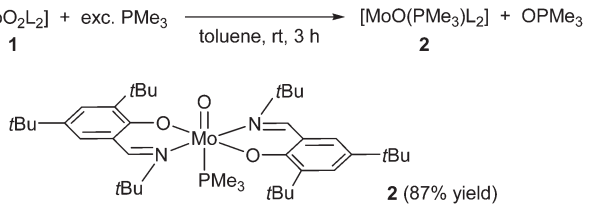

Scheme 2 Synthesis of molybdenum(IV) complex **2**.

Reactivity of the dioxo complex **1** in oxygen atom transfer (OAT) reactions was studied using trimethylphosphine and triphenylphosphine as oxygen acceptor substrates, allowing easy monitoring by ^{31}P NMR spectroscopy. Complex **1** was first reacted with an excess (4–5 equiv.) trimethylphosphine in toluene under inert conditions (Scheme 2).

The reaction was indicated by a quick change of color from deep orange to crimson and ^{31}P NMR measurements reveal the formation of $OPMe_3$ and further reduced molybdenum(IV) complex **2**. After evaporation of the solvent and excess PMe_3 then re-dissolution of the crude material in cold heptane, $OPMe_3$ is removed *via* subsequent filtration over a pad of Celite. The pure reduced complex **2** was isolated as a highly sensitive to moisture and air, crimson solid in excellent yield (87%). Interestingly, ^{1}H and ^{13}C NMR spectra revealed the formation of a symmetric compound as only one set of resonances for both coordinate ligands is observed (Table 1). Characteristic signals in the ^{1}H NMR spectrum in benzene-d_6 are given at 8.33 ppm (imine proton), 7.42 and 7.19 ppm (aromatic protons). The ^{31}P NMR spectrum of a concentrated solution of **2** in benzene-d_6 points to the existence of a single Mo–PMe_3 species (−9.47 ppm) further evidenced by the occurrence of a doublet at 0.91 ppm with the integration of nine protons in the ^{1}H NMR spectrum.

The symmetric coordination in complex **2** has not been described in the literature up to now. In such type of OAT reactions, either the formation of a dimeric Mo(V)–O–Mo(V) species is observed, or the free coordination site is captured by a phosphine in *cis* position to the $[MoO]^{2+}$ metal core, forming complexes of the type $[MoO(PR_3)L_2]$[12,15,21] or $[MoO(OPR_3)L_2]$.[22] Such complexes render the geometry around the metal center non-symmetric and therefore lead to two sets of resonances

Table 1 ^{1}H NMR characteristic signals shifts in ppm for complexes **1**, **2**, **3** and **4** in benzene-d_6

Compd.	Ar–C*H*N	Ar–*H*	Ar–*H*
1	8.33	7.66	7.15
2	8.32	7.40	7.16
3	8.21	7.47	7.24
4	8.63, 8.55	7.60, 7.49	7.19, 7.19

Open Access Article. Published on 09 November 2015. Downloaded on 1/25/2026 11:42:48 AM.
This article is licensed under a Creative Commons Attribution 3.0 Unported Licence.

for both coordinate ligands in NMR analysis. Our results point to the symmetric coordination of the PMe_3 molecule in *trans* position to the Mo=O moiety. Although an equilibrium between a *trans* and *cis* species is in principle feasible, this is very unlikely as we observe narrow peaks in NMR spectroscopy. Furthermore, low temperature ^{31}P NMR spectroscopy in toluene-d_8 at −30 °C shows only one signal (see ESI†). This unusual arrangement is presumably caused by the high steric demand of the ligand. Two isomers are conceivable with the phosphine and the oxo groups *trans* to each other, namely the *trans*-N,N isomer depicted in Scheme 2 and the *trans*-N,O isomer, but the latter seems sterically too congested to exist.

ESI-MS measurements and elemental analysis corroborates the formation of a monomeric $[MoO(PMe_3)L_2]$ complex. Information about the molecular size of the complex were obtained from 2D DOSY diffusion measurements on a sample containing complex **2** and free ligand in benzene-d_6. For the free ligand (HL), a diffusion coefficient $D = -8.805$ ($\log(m^2\ s^{-1})$) corresponding to 1.57×10^{-9} $m^2\ s^{-1}$ was found, while complex **2** diffuses with a $D = -8.878$ ($\log(m^2\ s^{-1})$) corresponding to 1.32×10^{-9} $m^2\ s^{-1}$. Based on the Stokes–Einstein equation, the relative hydrodynamic radii of two components are related to the diffusion coefficients by $D_1/D_2 = r_2/r_1$. Therefore, the experimental diffusions coefficients of complex **2** and free ligand correspond to relative hydrodynamic radii of 1.18 : 1. Such an increase of 18% of the diameter of the complex relative to HL can only be explained by a monomer. In addition, the DOSY analysis of a sample containing the dioxo complex **1** and the reduced complex **2** showed similar diffusion for both complexes (see ESI†).

The OAT reaction of complex **1** with 2 equiv. PPh_3 in benzene-d_6 at room temperature as well results in a color change from deep orange to purple. After 5 h under stirring, an NMR sample was taken. ^1H and ^{13}C NMR spectra exhibited again one set of resonances for both coordinate ligands, indicating formation of a new symmetric compound $[MoOL_2]$ **3**. Characteristic signals in ^1H NMR in benzene-d_6 (Table 1) are given at 8.21 ppm (imine proton), 7.47 and 7.24 ppm (aromatic protons). ^{31}P NMR confirmed formation of $OPPh_3$ (signal at 24.78 ppm) but showed that the other equivalent of PPh_3 does not coordinate the molybdenum center and thus remains free (signal at 5.41 ppm). Evaporation of the solvent led to a highly air sensitive purple powder which contains **3**, $OPPh_3$ and PPh_3. Removal of $OPPh_3$ was performed by filtration of a heptane solution of the mixture over dry Celite, which however did not remove residual PPh_3. Thus, sublimation of residual PPh_3 at 100 °C was attempted to isolate **3**, but only lead to decomposition of the complex. Nevertheless, its sensitivity towards air as well as ^1H and ^{31}P NMR spectroscopy lead us to believe that the monooxo $[MoOL_2]$ complex **3** is formed *in situ* rather than a Mo(v) dimer or a Mo(iv) phosphino species. The monomeric structure of **3** was confirmed by DOSY analysis, with a diffusion coefficient similar to that obtained for complex **2**.

Although complexes with the $[MoO(O_2)]^{2+}$ or $[MoO(O_2)_2]^{2+}$ cores are relatively abundant in the literature, as complexes thereof are available from the reaction of $[MoO_3]$ and the appropriate ligand in aqueous H_2O_2,[23] the activation of molecular oxygen by molybdenum compounds is scarce in the literature. As previously described by our group, re-oxidation of the molybdenum(iv) complex type $[MoO(PMe_3)L_2]$ with molecular oxygen either results in the formation of $[MoO_2]^{2+}$ or $[MoO(O_2)]^{2+}$ complexes,[12,15] depending on the steric demand in the ligand backbone. When benzene-d_6 solutions of **2** and **3** were exposed to dry molecular oxygen, color change from crimson to orange for complex **2** and from purple to orange for **3** occurred. ^1H and ^{13}C NMR spectra indicate the formation of the same, non-symmetric compound in both reactions, as two sets of resonances for both coordinated ligands are observed (*e.g.* in the ^1H NMR spectra 2 × Ar–C*H*N at 8.55 and 8.63 ppm, Table 1). Such behavior is in good accordance to the literature regarding the formation of a $[MoO(O_2)]$-type complex, as the coordination of the O_2 molecule in *cis* position to the $[MoO]^{2+}$ renders the geometry around the metal center non-symmetric.[16] It is noteworthy that this $[MoO(O_2)L_2]$ complex **4** can be synthesized directly by reacting **1** with a 5-fold excess phosphine under O_2 atmosphere. After purification, **4** was isolated as an orange solid in 93% yield (Scheme 3).

Single crystals suitable for X-ray diffraction analyses of complex **4** were obtained from concentrated THF solutions layered with pentane at room temperature. Crystal data and structure refinements are presented in the Experimental section. The structure reveals a hepta-coordinated metal center in a distorted pentagonal bi-pyramidal geometry (Fig. 2). The metal center is ligated by one terminal oxygen atom, a η^2-peroxo moiety and two bidentate Schiff base ligands. The terminal oxygen atom is found to be in *cis* position to the η^2-peroxo moiety. All these features as well as bonds lengths and angles values are in good accordance with similar $[MoO(O_2)]^{2+}$ complexes reported previously in the literature.[10,12,24]

The re-oxidation of the reduced $[MoO(PMe_3)L_2]$ complex **2** with molecular O_2, yielding the $[MoO(O_2)L_2]$ complex **4** (Scheme 3), provided an interesting information. The ^{31}P NMR spectra measured directly after exposition of **2** to O_2 showed that the phosphine attached to the Mo is released as a free phosphine when **4** is formed. The same NMR sample, maintained under O_2 atmosphere was submitted again for analysis after 24 h. The ^{31}P NMR spectra revealed that the equivalent of

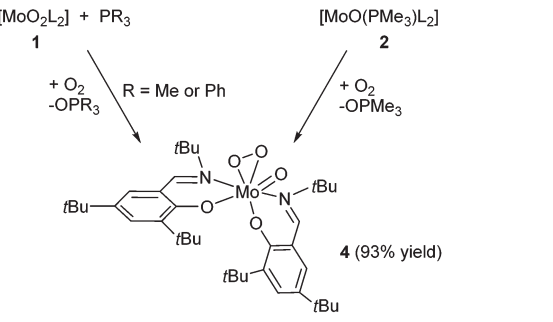

Scheme 3 Synthesis of the oxo–peroxo Mo(vi) complex **4**.

 This journal is © The Royal Society of Chemistry 2015

Open Access Article. Published on 09 November 2015. Downloaded on 1/25/2026 11:42:48 AM.
This article is licensed under a Creative Commons Attribution 3.0 Unported Licence.

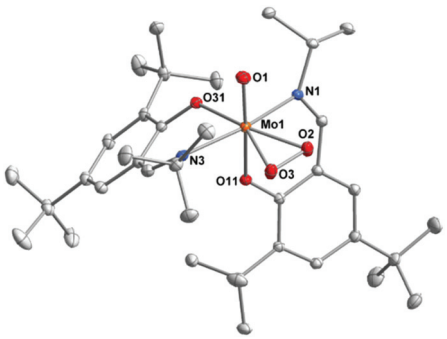

Fig. 2 Molecular structure of complex **4**. Thermal ellipsoids have been drawn at 50% probability level. Hydrogen atoms are omitted for clarity. Selected bond lengths (Å) and angles (°): Mo1–O1 1.6909(10); Mo1–O2 1.9487(10); Mo1–O3 1.9447(10); Mo1–O11 2.0494(9); Mo1–O31 2.0269(9); Mo1–N1 2.2548(11); Mo1–N2 2.2162(11); O2–O3 1.4332(13); O1–Mo1–O11 170.37(4); O2–Mo1–O31 155.69(4); O3–Mo1–O31 153.96(4); N1–Mo1–N3 165.72(4); O1–Mo1–O2 99.17(5); O1–Mo1–O3 101.82(5); O1–Mo1–O31 91.99(4); O1–Mo1–N1 91.57(4).

free PMe_3 formed during the re-oxidation had been converted to $OPMe_3$. Thus, when **2** reacted with O_2 as presented in Scheme 3, substitution of the phosphine by O_2 occurred and only subsequently PMe_3 was oxidized to $OPMe_3$ by the complex **4** (see Fig. S3 in ESI†). These observations are noteworthy as phosphine is usually strongly coordinated, so that prior oxidation is required for its displacement. Here, the steric demand of the ligand and the *trans*-effect resulting from the presence of the oxo group leads to a weakly coordinated PMe_3 rendering the system reactive. Such labilization of phosphine ligands due to a *trans*-effect was already observed with other Mo complexes.[25] The fact that the free PMe_3 equivalent could be oxidized under O_2 atmosphere in presence of **4** lead us to investigate the role of the oxo–peroxo complex as possible catalyst for the oxidation of phosphine using O_2, as described thereafter. In order to exclude auto oxidation of PMe_3 and to prove the reactivity of the oxo–peroxo complex in OAT, the reaction of **4** with 2 equiv. PMe_3 in exclusion of O_2 was investigated (Scheme 4). Monitoring the reaction by ^1H and ^{31}P NMR spectroscopy revealed that the oxo–peroxo complex **4** is able to oxidize tertiary phosphines, but more importantly that both atoms of the peroxo group are involved in this transfer. Although the reaction does not go to completion, ^1H NMR spectra show formation of a new molybdenum species and $OPMe_3$ in a 1 : 2 ratio, along with unreacted PMe_3 and complex **4**. As shown in Fig. 3, after t = 5 h approx. 25% conversion is observed and after t = 30 h 50%. This Mo intermediate exhibits a single set of signal very similar to that of the Mo(IV) monooxo complex **2** (*e.g.* signals at 8.34, 7.40 and 7.21 ppm). The small differences between the ^1H NMR signals of the observed Mo intermediate and **2** can be explained by differences in the coordination of the phosphine. In the intermediate, PMe_3 is only weakly interacting with Mo but is not fully coordinated. This explanation is supported by the ^1H NMR signal of the weakly interacting PMe_3 (0.86 ppm, J_{P-C} = 4.2 Hz), which is different from free PMe_3 (0.81 ppm, J_{P-C} < 2 Hz) and from the fully bound PMe_3 in **2** (0.91 ppm, J_{P-C} = 7 Hz). During the course of the reaction, no formation of a plausible Mo(VI) dioxo intermediate (complex **1**) was observed, indicating that the transfer of the first oxygen atom from the peroxo unit is the rate determining step of the process, while transfer of the second oxygen atom is either concerted or occurs much faster. This was corroborated by kinetic experiments using UV-Vis spectroscopy. The OAT reaction from complex **1** with a 100-fold excess PMe_3 (pseudo-first order conditions) to form the reduced complex **2** was found to have a rate constant k = 0.003 s^{-1}. The corresponding reaction of complex **4** with 100 equiv. PMe_3 and the same concentration for the complex and phosphine was found to be orders of magnitude slower as hardly any reaction occurred in the observed timeframe (see ESI†).

As both the dioxo and oxo–peroxo complexes are active in OAT reaction, catalytic oxidation of PMe_3 was investigated. In the literature, the molybdenum complexes which activate O_2 could not catalytically oxidize phosphines. $[MoO(O_2)(CN)_4][PPh_4]_2$ is capable of oxidizing 3 mol PPh_3 per 2 mol molybdenum in the presence of molecular O_2,[10] but no further oxidation of PPh_3 was obtained due to conproportionation of the dioxo Mo(VI) and the monoxo Mo(IV) intermediates. Although PMe_3 is easily oxidized without any metal in presence of water and air, the stability of PMe_3 against dry O_2 in dry benzene-d_6 solutions was confirmed by running a blank experiment (see ESI†). For the catalytic run, a solution of **1** (10 mg, 14 μmol) in benzene-d_6 was prepared and placed under O_2 atmosphere. Then 100 equivalents PMe_3 were added and the reaction was left to stir for 24 h (Scheme 5). The reaction was monitored by ^1H and ^{31}P NMR analysis. Integration of PMe_3 and $OPMe_3$ signals after 24 h showed the conversion of 19 equivalents PMe_3 to $OPMe_3$. After evaporation of the solvent and unreacted phosphine, mass balance confirmed formation of $OPMe_3$ besides the residue of the catalyst. Control experiments in the presence of sodium molybdate or $[MoO_2(acac)_2]$ did not lead to formation of $OPMe_3$. The reactivity of **1** is limited by

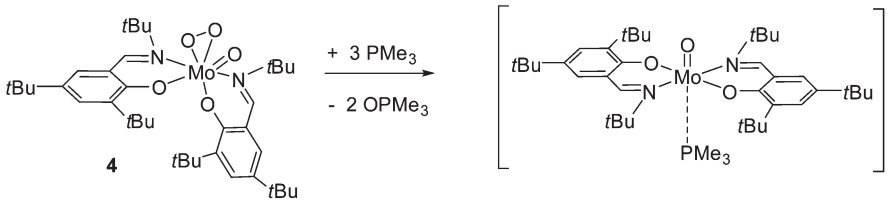

Scheme 4 OAT reaction of the oxo–peroxo complex **4** in exclusion of O_2 in benzene-d_6.

Open Access Article. Published on 09 November 2015. Downloaded on 1/25/2026 11:42:48 AM.
This article is licensed under a Creative Commons Attribution 3.0 Unported Licence.

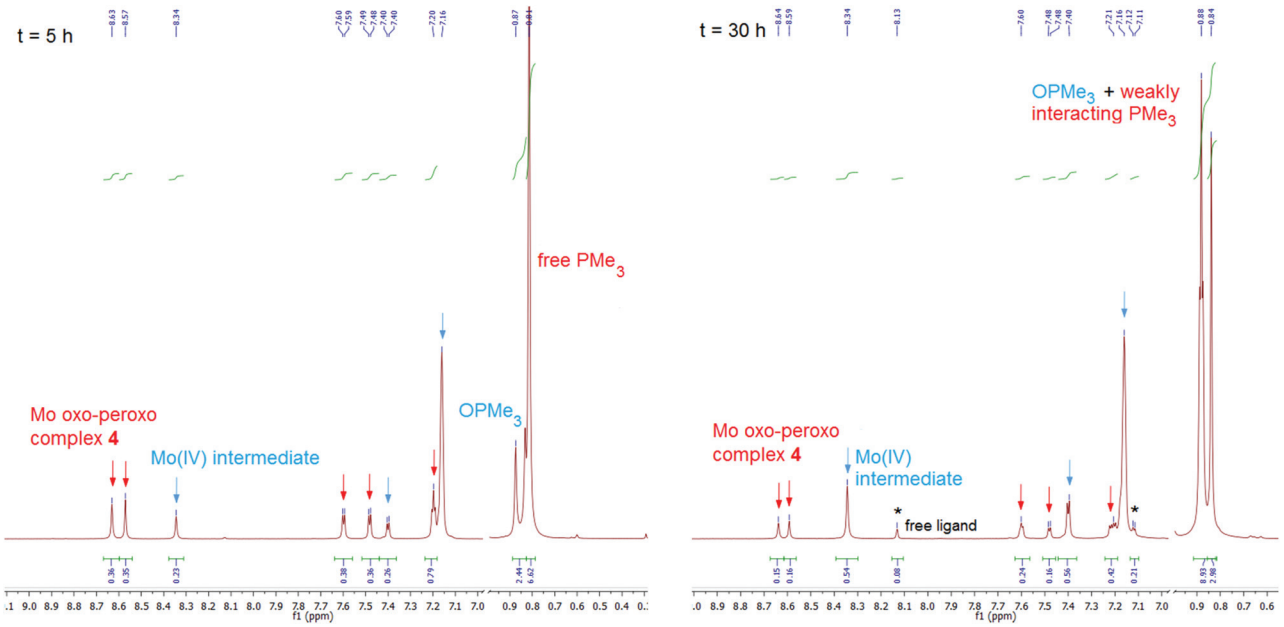

Fig. 3 ^{1}H NMR spectra in benzene-d_6 at t = 5 h (left) and t = 30 h (right) of the reaction of molybdenum oxo–peroxo complex **4** with 2 equiv. PMe_3 under O_2 exclusion.

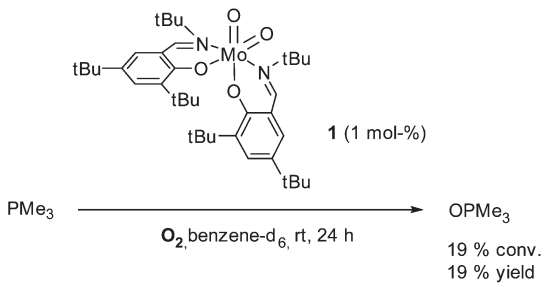

Scheme 5 Conversion of PMe_3 to $OPMe_3$ catalyzed by **1** using O_2.

decomposition of the complex, but is a successful progress toward the use of molecular oxygen as sole oxidant in catalytic OAT reactions.

Conclusion

We were able to prepare a new molybdenum(VI) dioxo complex **1** which is active in oxygen atom transfer reaction to tertiary phosphines, allowing the isolation of the unusual *trans*-[MoO(PMe$_3$)L$_2$] complex **2**. The activation of molecular oxygen by the reduced species yields the oxo–peroxo complex [MoO(O$_2$)L$_2$] **4** in excellent yield. **4** is also active in OAT and NMR spectroscopy studies show that both atoms of the peroxo group are transferred to phosphine. Hence, the molybdenum (VI) dioxo complex **1** exhibits promising results as catalyst for oxidations using O_2 as the oxidant.

Experimental section

All reactions have been carried out under nitrogen using standard Schlenk or glovebox techniques. [MoO_2Cl_2] was purchased from Sigma-Aldrich and used in the Glovebox without further purification. The Schiff base ligand was synthesized according to previously published literature.[19] Solvents were purified *via* a Pure-Solv MD-4-EN solvent purification system from Innovative Technology, Inc. The ^{1}H and ^{13}C NMR spectra were recorded on a Bruker Optics Instrument 300 MHz. Peaks are denoted as singlet (s), doublet (d), doublet of doublets (dd), triplet (t) and multiplet (m), Ar denotes aromatic protons. Chemical shifts are reported in ppm and are referenced using the residual solvent peak. To obtain self-diffusion coefficients we used two-dimensional diffusion ordered spectroscopy (DOSY).[26] The employed pulse sequence was a bipolar pulse pair longitudinal eddy current delay (BPP-LED) sequence, using 32 scans per increment, 60 ms diffusion delay time, 1 ms gradient pulses and variation of the gradient strength in 32 increments, linearly varied between 2 and 95% of maximum (which is 53.5 G cm^{-1}). DOSY analysis was performed using the Bruker DOSY package of TopSpin 3.1. All DOSY measurements were carried out at 300 K on a Bruker Avance III 500 MHz NMR spectrometer using a 5 mm TXI probe with z-axis gradients. IR spectra were measured as solid samples on a Bruker Alpha P Diamond FTIR-ATR spectrometer or as liquid samples in benzene on a Bruker FT-MIR matrix MF *in situ* spectrometer using a glass fiber optic probe. ESI-MS spectra were recorded in acetonitrile on an Agilent 1100 Series LCMSD (SL type). Elemental analyses were carried out using a Heraeus Vario Elementar automatic analyzer at the Institute of Inorganic Chemistry at the University of Technology in Graz.

This journal is © The Royal Society of Chemistry 2015

Open Access Article. Published on 09 November 2015. Downloaded on 1/25/2026 11:42:48 AM.
This article is licensed under a Creative Commons Attribution 3.0 Unported Licence.

$[MoO_2L_2]$ (1)

Ligand HL (500 mg, 1.7 mmol, 2 equiv.) was dissolved in 5 ml of dry toluene and slowly added to a suspension of $[MoO_2Cl_2]$ (180 mg, 0.9 mmol, 1 equiv.) in 5 mL of dry toluene under inert conditions. Dry triethylamine (0.26 mL, 1.9 mmol, 2.2 equiv.) was then added. The formation of the complex was immediately indicated by a quick change of color from pale yellow to deep red. To ensure complete complex formation, the solution was stirred 5 h at room temperature. The mixture was then filtered with a cannula and the solvent was removed *in vacuo*. The residue was washed thrice with 10 ml of cold pentane to afford complex **1** as an orange solid in 64% yield (407 mg). Single crystals suitable for X-ray diffraction analyses were obtained by slow evaporation from concentrated toluene solution at room temperature.

^{1}H NMR (300 MHz, benzene-d_6, ppm) δ = 8.33 (s, 1H, Ar–C*H*N), 7.66 (d, $^4J_{H-H}$ = 2.7 Hz, 1H, Ar–*H*), 7.15 (d, $^4J_{H-H}$ = 2.7 Hz, 1H, Ar–*H*), 1.56 (s, 9H, NC(CH_3)$_3$), 1.33 (s, 9H, Ar–C(CH_3)$_3$), 1.30 (s, 9H, Ar–C(CH_3)$_3$).

^{13}C NMR (75 MHz, benzene-d_6, ppm) δ = 167.48 (Ar–*C*HN), 164.31 (*Ar*–O), 139.32 (Ar), 139.00 (Ar), 131.03 (*Ar*–H), 129.28 (*Ar*–H), 123.39 (*Ar*), 64.96 (N*C*(CH$_3$)$_3$), 35.28 (Ar–*C*(CH$_3$)$_3$), 34.18 (Ar–*C*(CH$_3$)$_3$), 31.59 (Ar–C(*C*H$_3$)$_3$), 31.24 (N(*C*H$_3$)$_3$), 29.57 (Ar–C(*C*H$_3$)$_3$).

IR (ATR, cm^{-1}): ν = 1613 (m, C═N), 1587 (m, C═N), 1534 (m), 1387 (m), 1255 (m), 1169 (s), 913 (s, Mo═O), 883 (s, Mo═O), 836 (m), 745 (m), 533 (m).

Anal. Calcd for $MoO_4N_2C_{38}H_{60}$: C, 64.75; H, 8.58; N, 3.97. **Found**: C, 64.29; H, 8.42; N, 3.73%.

$[MoO(PMe_3)L_2]$ (2)

$[MoO_2L_2]$ (100 mg, 0.14 mmol, 1 equiv.) was dissolved in dry toluene and excess PMe_3 (70 μL, 0.7 mmol, 5 equiv.) was added. The OAT was indicated by a quick change of color from orange to dark red. After stirring for 3 hours, the solvent and excess PMe_3 were removed under reduced pressure. The obtained material was re-dissolved in cold dry heptane (5 mL) and filtered over a pad of Celite. After evaporation of the solvent, complex **2** was obtained as dark red solid. Yield: 95 mg (87%).

^{1}H NMR (300 MHz, benzene-d_6, ppm) δ = 8.32 (s, 2H, Ar–C*H*N), 7.40 (d, $^4J_{H-H}$ = 2.6 Hz, 2H, Ar–*H*), 7.16 (m, 2H, Ar–*H*), 1.65 (s, 18H, N–C(CH_3)$_3$), 1.34 (s, 18H, Ar–C(CH_3)$_3$), 1.31 (s, 18H, Ar–C(CH_3)$_3$), 0.91 (d, J_{P-H} = 7 Hz, 9H, OPMe$_3$).

^{13}C NMR (75 MHz, benzene-d_6, ppm) δ = 164.57 (Ar–*C*HN), 162.96 (*Ar*–O), 138.78 (*Ar*), 136.58 (*Ar*), 131.55 (*Ar*–H), 128.90 (*Ar*–H), 122.59 (*Ar*), 64.47 (N–*C*(CH$_3$)$_3$), 35.67 (Ar–*C*(CH$_3$)$_3$), 34.05 (Ar–*C*(CH$_3$)$_3$), 32.07 (Ar–C(*C*H$_3$)$_3$), 31.81 (N–C(*C*H$_3$)$_3$), 30.60 (Ar–C(*C*H$_3$)$_3$), 17.55 (d, J_{P-C} = 17.9 Hz, Mo–P(*C*H$_3$)$_3$).

^{31}P NMR (121 MHz, benzene-d_6, 298 K, ppm) δ −9.47 (Mo–*P*(CH$_3$)$_3$).

IR (FT-IR, benzene, cm^{-1}): ν 1605 (m, C═N), 1542 (m), 1460 (s), 1436 (s), 1396 (s), 1362 (m), 1307 (s), 1256 (s), 1165 (s), 932 (s, Mo═O), 836 (m).

ESI-MS (50 V) *m*/*z* (%): 690.3 (100) [M − HP(CH$_3$)$_3$].

Anal. Calcd for $MoO_3N_2PC_{41}H_{69}$: C, 64.38; H, 9.09; N, 3.66. Found: C, 64.25; H, 9.23; N, 3.38%.

$[MoOL_2]$ (3)

$[MoO_2L_2]$ (100 mg, 0.14 mmol, 1 equiv.) was dissolved in dry toluene and an excess PPh_3 (74 mg, 0.28 mmol, 2 equiv.) was added. The OAT was indicated by a quick change of color from orange to purple. After stirring for 15 hours, the solvent was removed under reduced pressure. The obtained material was re-dissolved in cold dry heptane (5 mL) and filtered over a pad of celite. After evaporation of the heptane, $[MoOL_2]$ was obtained as a purple solid in 60% yield, with partial decomposition to the free ligand and traces of triphenylposphine.

^{1}H NMR (300 MHz, benzene-d_6, ppm) δ = 8.21 (s, 2H, Ar–C*H*N), 7.47 (d, $^4J_{H-H}$ = 2.6 Hz, 2H, Ar–*H*), 7.24 (d, $^4J_{H-H}$ = 2.6 Hz, 2H, Ar–*H*), 1.61 (s, 18H, N–C(CH_3)$_3$), 1.34 (s, 18H, Ar–C(CH_3)$_3$), 1.33 (s, 18H, Ar–C(CH_3)$_3$).

^{13}C NMR (75 MHz, benzene-d_6, ppm) δ = 165.66 (Ar–*C*HN), 163.68 (*Ar*–O), 139.01 (*Ar*), 138.52 (*Ar*), 132.05 (*Ar*–H), 129.07 (*Ar*–H), 119.06 (*Ar*), 65.97 (N–*C*(CH$_3$)$_3$), 35.80 (Ar–*C*(CH$_3$)$_3$), 34.27 (Ar–*C*(CH$_3$)$_3$), 31.69 (Ar–C(*C*H$_3$)$_3$), 30.83 (N–C(*C*H$_3$)$_3$), 30.14 (Ar–C(*C*H$_3$)$_3$).

$[MoO(O_2)L_2]$ (4)

$[MoO_2L_2]$ (100 mg, 0.14 mmol, 1 equiv.) was dissolved in dry benzene (5 mL) followed by the addition of excess PMe_3 (53 mg, 70 μL, 0.70 mmol, 5 equiv.). The OAT was indicated by a quick change of color from orange to dark red. The solution was stirred for 30 minutes, followed by exposure of this solution to dry molecular oxygen for 5 minutes. The reaction solution quickly changed the color from dark violet to orange. The mixture was left to stir for 30 minutes and the solvent was removed *in vacuo*. The product was dissolved in heptane (5 mL) and twice filtered over a pad of Celite. $[MoO(O_2)L_2]$ was obtained as an orange solid. Yield: 87 mg (93%). For elemental analyses, the complex was dissolved in minimum amount of CH_2Cl_2 and again filtered over a pad of Celite. Single crystals suitable for X-ray diffraction analyses were obtained from concentrated THF solutions layered with pentane.

^{1}H NMR (300 MHz, benzene-d_6, ppm) δ = 8.63 (s, 1H, Ar–C*H*N), 8.55 (s, 1H, Ar–C*H*N), 7.60 (d, $^4J_{H-H}$ = 2.4 Hz, 1H, Ar–*H*), 7.49 (d, $^4J_{H-H}$ = 2.4 Hz, 1H, Ar–*H*), 7.19 (d, $^4J_{H-H}$ = 2.4 Hz, 2H, Ar–*H*), 1.87 (s, 9H, NC(CH_3)$_3$), 1.74 (s, 9H, NC(CH_3)$_3$), 1.41 (s, 9H, Ar–C(CH_3)$_3$), 1.27 (s, 9H, Ar–C(CH_3)$_3$), 1.23 (s, 9H, Ar–C(CH_3)$_3$), 1.09 (s, 9H, Ar–C(CH_3)$_3$).

^{13}C NMR (75 MHz, benzene-d_6, ppm) δ = 166.36 (overlapping signals, 2 × Ar–*C*HN), 161.74 (*Ar*–O), 159.65 (*Ar*–O), 140.22 (*Ar*), 139.79 (*Ar*), 138.97 (*Ar*), 137.78 (*Ar*), 131.83 (*Ar*–H), 130.86 (*Ar*–H), 130.16 (*Ar*–H), 130.37 (*Ar*–H), 124.45 (*Ar*), 122.63 (*Ar*), 67.96 (N*C*(CH$_3$)$_3$), 67.49 (N*C*(CH$_3$)$_3$), 35.44 (Ar–*C*(CH$_3$)$_3$), 34.77 (Ar–*C*(CH$_3$)$_3$), 34.13 (Ar–*C*(CH$_3$)$_3$), 34.06 (Ar–*C*(CH$_3$)$_3$), 32.78 (NC(*C*H$_3$)$_3$), 31.60 (NC(*C*H$_3$)$_3$), 31.54 (2 × Ar–C(*C*H$_3$)$_3$), 30.25 (Ar–C(*C*H$_3$)$_3$), 29.91 (Ar–C(*C*H$_3$)$_3$).

IR (ATR, cm^{-1}): ν 1606 (s, C═N), 1541 (m), 1255 (s), 1168 (s), 931 (s, Mo═O), 838 (s), 777 (s), 747 (m), 542 (s, Mo–O).

Open Access Article. Published on 09 November 2015. Downloaded on 1/25/2026 11:42:48 AM.
This article is licensed under a Creative Commons Attribution 3.0 Unported Licence.

Anal. Calcd for $MoO_5N_2C_{38}H_{60}\cdot 0.23\ CH_2Cl_2$: C, 62.00; H, 8.23; N, 3.78. **Found**: C, 62.18; H, 8.44; N, 3.90%.

Oxygen atom transfer reactivity of $[MoO(O_2)L_2]$ (4)

$[MoO(O_2)L_2]$ (25 mg, 0.035 mmol, 1 equiv.) was dissolved in dry benzene-d_6 under inert conditions in a Young NMR tube. 2 equivalent PMe_3 (8 μL, 0.07 mmol) was added using a micropipette. The OAT reaction was monitored by ^1H and ^{31}P NMR spectroscopy.

Catalytic oxidation of trimethylphosphine

$[MoO_2L_2]$ (complex **1**, 10 mg, 14 μmol) was placed in a Schlenk flask in the glovebox. The Schlenk flask was evacuated then refilled with dry O_2. Dry benzene-d_6 (2 mL) and trimethylphosphine (108 mg, 0.15 μL, 1.4 mmol, 100 equiv.) were added and the reaction was left to stir under O_2 atmosphere for 24 h. The reaction was monitored by ^1H and ^{31}P NMR at t = 4 h, 20 h and 24 h. After removal of the solvent, the mass balance was calculated and the yield of $OPMe_3$ confirmed by integration of the signals in the ^1H NMR spectrum at t = 24 h (yield = 19%). To confirm the stability of PMe_3 under O_2 atmosphere, a blank experiment was performed. A Schlenk flask was evacuated then refilled with dry O_2. Dry benzene-d_6 (2 mL) and trimethylphosphine (108 mg, 0.15 μL, 1.4 mmol, 100 equiv.) were added and the reaction was left to stir under O_2 atmosphere for 24 h. The reaction was monitored by ^1H and ^{31}P NMR at t = 4 h, 20 h and 24 h. at t = 24 h, a signal for $OPMe_3$ could be observed in the ^1H NMR (1% yield) but no signal was observed in ^{31}P NMR. After 24 h, the solvent and free PMe_3 were evaporated, no solid $OPMe_3$ could be isolated.

OAT kinetic study

In the glovebox, a solution of 7 mg of complex **1** in 5 mL toluene (2×10^{-3} mol L^{-1}) and a solution of 15 mg PMe_3 in 1 mL toluene (0.2 mol L^{-1}) were prepared. Using a micropipette, 100 μL of the solution containing the complex were placed in a quartz cuvette and 2 mL toluene were added. Then 100 μL of the solution containing PMe_3 were added and the cuvette was sealed with a Teflon stopper and parafilm. The sample was removed from the glovebox and the measurement immediately started. The reaction was monitored by the dissapearance of the signal at 430 nm, at room temperature using a Cary50 Conc. UV-Vis spectrophotometer under PC control using the kinetics program "Scan" included with the instrument software. The same procedure was followed preparing a solution of 7 mg of complex **4** in 5 mL toluene (2×10^{-3} mol L^{-1}).

Structure determination

For X-ray structure analyses the crystals were mounted onto the tip of glass fiber and data collection was performed at 100 K using graphite monochromated Mo K_α radiation (λ = 0.71073 Å) with a BRUKER-AXS SMART APEX II diffractometer equipped with a CCD detector. Essential details of the crystal-data and structure refinements for compounds **1** and **4** are summarized in Table 2. Crystallographic data for the structures of compounds **1** and **4** have been deposited with the Cambridge Crystallographic Data Center [CCDC 1413968 for **1**, CCDC 1413969 for **4**].

Table 2 Crystallographic data and structure refinements for complexes **1** and **4**

	1	**4**
Empirical formula	$C_{38}H_{60}MoN_2O_4$	$2MoO_5N_2C_{38}H_{60}\cdot xC_4H_8O\cdot(1-x)C_5H_{12}$; x = 0.786(6)
Formula weight	704.82	1513.75
Crystal description	Plate, red	Block, red
Crystal size (mm)	0.27 × 0.17 × 0.05 mm	0.32 × 0.25 × 0.25
Crystal system, space group	Monoclinic, $P21/n$	Monoclinic, $C2/c$
Unit cell dimensions		
a (Å)	10.3863(4)	24.3085(13)
b (Å)	11.4627(5)	15.8102(8)
c (Å)	33.1945(13)	20.8035(11)
α (°)	90	90
β (°)	98.6499(17)	94.112(2)
γ (°)	90	90
Volume (Å^3)	3907.0(3)	7974.7(7)
Z, calculated density (g cm^{-3})	4, 1.198	4, 1.261
F(000)	1504	3233.9
Linear absorption coefficient μ (mm^{-1})	0.373	0.373
Absorption correction	Semi-empirical from equiv.	Semi-empirical from equiv.
Temperature (K)	100	100
Wavelength (Mo K_α) (Å)	0.71073	0.71073
Theta range for data collection (°)	2.46 to 28.45	1.79 to 30.00
Limiting indices	$-12 \le h \le 12$ $-5 \le k \le 14$ $-40 \le l \le 40$	$-34 \le h \le 29$ $-22 \le k \le 22$ $-29 \le l \le 29$
Reflections collected/ unique	26 791/7661	46 647/11 648
Reflections with $I > 2\sigma(I)$	5550	10 882
R(int), R(sigma)	0.0549, 0.0723	0.0187, 0.0148
Completeness to theta max.	0.999	0.999
Refinement method	Full matrix least squares on F^2	Full matrix least squares on F^2
Data/restraints/ parameters	7661/432/0	11 648/486/12
Goodness-of-fit on F^2	1.107	1.100
Final R_1 wR_2 [$I > 2\sigma(I)$]	R_1 = 0.0585 wR_2 = 0.1401	R_1 = 0.0277 wR_2 = 0.0689
R indices (all data)	R_1 = 0.0869 wR_2 = 0.1507	R_1 = 0.0304 wR_2 = 0.0709
Largest diff. peak and hole (e Å^{-3})	1.484 and −2.767	1.283 and −0.599

Crystal structure determination of 1. The structure was solved by direct methods (SHELXS-97) and refined by full-matrix least-squares techniques against F^2 (SHELXL-2014/6). The non-hydrogen atoms were refined with anisotropic displacement parameters without any constraints. The H atoms of the phenyl rings as well as the H atoms bonded to the C atom of a C=N double bond were put at the external bisectors of the C–C–X angles at C–H distances of 0.95 Å and common isotropic displacement parameters were refined for these H atoms of the same ligand. The H atoms of the methyl groups were refined with common isotropic displacement parameters

 This journal is © The Royal Society of Chemistry 2015

Open Access Article. Published on 09 November 2015. Downloaded on 1/25/2026 11:42:48 AM.
This article is licensed under a Creative Commons Attribution 3.0 Unported Licence.

for the H atoms of the same *tert*-butyl group and idealized geometries with tetrahedral angles, enabling rotation around the C–C bonds, and C–H distances of 0.98 Å.

Crystal structure determination of 4. The structure could be solved (SHELXS-97) by interpretation of the patterson map (second solution) in the non-centrosymmetric space group *C*2, but not in centrosymmetric *C*2/*c*. After completion of the molecule an inversion center could be detected and the structure was refined by full-matrix least-squares techniques against F^2 (SHELXL-2014/6) in the centric space group *C*2/*c* after an appropriate shift of the origin. A void of approx. 188 Å^3 is occupied by a THF molecule disordered over two orientations lying near a center of symmetry or by a *n*-pentane molecule at the inversion center. The ratio of the refined occupation factors is 0.768(6) to 0.232(6). The non-hydrogen atoms of the solvent molecules were refined with isotropic displacement parameters with some restraints. The H atoms of the solvent molecules were included at calculated positions with their isotropic displacement parameters fixed to 1.2 times U_{eq} of the C atom they are bonded to. The non-hydrogen atoms of the metal complex were refined with anisotropic displacement parameters without any constraints. The H atoms of the phenyl rings were put at the external bisectors of the C–C–C angles at C–H distances of 0.95 Å and common isotropic displacement parameters were refined for the H atoms of the same ring. The H atoms H10 and H30 were put at the external bisector of the C–C–C angle at a C–H distance of 0.95 Å but the individual isotropic displacement parameters were free to refine. The H atoms of the methyl groups were refined with common isotropic displacement parameters for the H atoms of the same group and idealized geometries with tetrahedral angles, enabling rotation around the C–C bond, and C–H distances of 0.98 Å.

Acknowledgements

The authors gratefully acknowledge financial support from the Austrian Science Fund (FWF): project number P26264 and from NAWI Graz.

Notes and references

1 M. Amini, M. M. Haghdoost and M. Bagherzadeh, *Coord. Chem. Rev.*, 2013, **257**, 1093.
2 M. Schubert, J. Leppin, K. Wehming, D. Schollmeyer, K. Heinze and S. R. Waldvogel, *Angew. Chem., Int. Ed.*, 2014, **53**, 2494; R. Sanz and M. Pedrosa, *Curr. Org. Synth.*, 2009, **6**, 239.
3 R. Hille, *Dalton Trans.*, 2013, **42**, 3029; M. J. Romão, *Dalton Trans.*, 2009, 4053; R. H. Holm, *Coord. Chem. Rev.*, 1990, **100**, 183; R. Hille, *Trends Biochem. Sci.*, 2002, **27**, 360.
4 F. J. Hine, A. J. Taylor and C. D. Garner, *Coord. Chem. Rev.*, 2010, **254**, 1570; P. Basu and S. J. N. Burgmayer, *Coord. Chem. Rev.*, 2011, **255**, 1016; R. Hille, J. Hall and P. Basu, *Chem. Rev.*, 2014, **114**, 3963.
5 J. H. Enemark, J. J. A. Cooney, J.-J. Wang and R. H. Holm, *Chem. Rev.*, 2004, **104**, 1175; H. Sugimoto and H. Tsukube, *Chem. Soc. Rev.*, 2008, **37**, 2609; C. Schulzke, *Eur. J. Inorg. Chem.*, 2011, 1189; R. H. Holm, E. I. Solomon, A. Majumdar and A. Tenderholt, *Coord. Chem. Rev.*, 2011, **255**, 993; S. J. N. Burgmayer, M. Kim, R. Petit, A. Rothkopf, A. Kim, S. Bel Hamdounia, Y. Hou, A. Somogyi, D. Habel-Rodriguez, A. Williams and M. L. Kirk, *J. Inorg. Biochem.*, 2007, **101**, 1601; J. M. Berg and R. H. Holm, *J. Am. Chem. Soc.*, 1985, **107**, 925; A. Majumdar and S. Sarkar, *Coord. Chem. Rev.*, 2011, **255**, 1039.
6 J. Kollar, *US* 3351635, 1967; M. N. Sheng and J. G. Zajacek, *GB* 1136923, 1965; J.-M. Brégeault, *Dalton Trans.*, 2003, 3289; S. Shylesh, M. Jia and W. R. Thiel, *Eur. J. Inorg. Chem.*, 2010, 4395.
7 S. A. Hauser, M. Cokoja and F. E. Kühn, *Catal. Sci. Technol.*, 2013, **3**, 552.
8 I. W. C. E. Arends and R. A. Sheldon, in *Modern Oxidation Methods*, ed. J.-E. Bäckvall, Wiley-VCH Verlag GmbH & Co. KGaA, Weinheim, Germany, 2010, pp. 147–185; W. B. Tolman, *Activation of small molecules. Organometallic and bioinorganic perspectives*, Wiley-VCH Verlag GmbH & Co. KGaA, Weinheim, Germany, 2006.
9 J. Serrano-Plana, I. Garcia-Bosch, A. Company and M. Costas, *Acc. Chem. Res.*, 2015, **48**, 2397; W. Nam, *Acc. Chem. Res.*, 2015, **48**, 2415; E. I. Solomon, D. E. Heppner, E. M. Johnston, J. W. Ginsbach, J. Cirera, M. Qayyum, M. T. Kieber-Emmons, C. H. Kjaergaard, R. G. Hadt and L. Tian, *Chem. Rev.*, 2014, **114**, 3659; K. Ray, F. F. Pfaff, B. Wang and W. Nam, *J. Am. Chem. Soc.*, 2014, **136**, 13942; P. Comba, Y.-M. Lee, W. Nam and A. Waleska, *Chem. Commun.*, 2014, **50**, 412; K. E. Dalle, T. Gruene, S. Dechert, S. Demeshko and F. Meyer, *J. Am. Chem. Soc.*, 2014, **136**, 7428; P. Haack and C. Limberg, *Angew. Chem., Int. Ed.*, 2014, **53**, 4282; C. E. MacBeth, A. P. Golombek, V. G. Young Jr., C. Yang, K. Kuczera, M. P. Hendrich and A. S. Borovik, *Science*, 2000, **289**, 938; E. I. Solomon, P. Chen, M. Metz, S.-K. Lee and A. E. Palmer, *Angew. Chem., Int. Ed.*, 2001, **40**, 4570.
10 H. Arzoumanian, J. F. Petrignani, M. Pierrot, F. Ridouane and J. Sanchez, *Inorg. Chem.*, 1988, **27**, 3377.
11 J. Tachibana, T. Imamura and Y. Sasaki, *J. Chem. Soc., Chem. Commun.*, 1993, 1436; M. Minato, D.-Y. Zhou, K.-i. Sumiura, Y. Oshima, S. Mine, T. Ito, M. Kakeya, K. Hoshino, T. Asaeda, T. Nakada and K. Osakada, *Organometallics*, 2012, **31**, 4941.
12 G. Lyashenko, G. Saischek, A. Pal, R. Herbst-Irmer and N. C. Mösch-Zanetti, *Chem. Commun.*, 2007, 701.
13 C. Y. Lorber, S. P. Smidt and J. A. Osborn, *Eur. J. Inorg. Chem.*, 2000, 655.
14 M. A. Katkar, S. N. Rao and H. D. Juneja, *RSC Adv.*, 2012, **2**, 8071; S. N. Rao, N. Kathale, N. N. Rao and K. N. Munshi, *Inorg. Chim. Acta*, 2007, **360**, 4010; W. A. Herrmann, G. M. Lobmaier, T. Priermeier, M. R. Mattner and B. Scharbert, *J. Mol. Catal. A: Chem.*, 1997, **117**, 455.

Open Access Article. Published on 09 November 2015. Downloaded on 1/25/2026 11:42:48 AM.
This article is licensed under a Creative Commons Attribution 3.0 Unported Licence.

15 G. Lyashenko, G. Saischek, M. E. Judmaier, M. Volpe, J. Baumgartner, F. Belaj, V. Jancik, R. Herbst-Irmer and N. C. Mösch-Zanetti, *Dalton Trans.*, 2009, 5655.
16 M. E. Judmaier, C. Holzer, M. Volpe and N. C. Mösch-Zanetti, *Inorg. Chem.*, 2012, **51**, 9956.
17 T. Arumuganathan, M. Volpe, B. Harum, D. Wurm, F. Belaj and N. C. Mösch-Zanetti, *Inorg. Chem.*, 2012, **51**, 150; M. Volpe and N. C. Mösch-Zanetti, *Inorg. Chem.*, 2012, **51**, 1440; J. A. Schachner, P. Traar, C. Sala, M. Melcher, B. N. Harum, A. F. Sax, M. Volpe, F. Belaj and N. C. Mösch-Zanetti, *Inorg. Chem.*, 2012, **51**, 7642; M. E. Judmaier, C. H. Sala, F. Belaj, M. Volpe and N. C. Mösch-Zanetti, *New J. Chem.*, 2013, **37**, 2139; N. C. Mösch-Zanetti, D. Wurm, M. Volpe, G. Lyashenko, B. Harum, F. Belaj and J. Baumgartner, *Inorg. Chem.*, 2010, **49**, 8914.
18 S. K. Sharma, P. S. May, M. B. Jones, S. Lense, K. I. Hardcastle and C. E. MacBeth, *Chem. Commun.*, 2011, **47**, 1827; W.-D. Wang and J. H. Espenson, *Inorg. Chem.*, 2001, **40**, 1323; B. G. Jacobi, D. S. Laitar, L. Pu, M. F. Wargocki, A. G. DiPasquale, K. C. Fortner, S. M. Schuck and S. N. Brown, *Inorg. Chem.*, 2002, **41**, 4815.
19 G. Alesso, M. Sanz, M. E. G. Mosquera and T. Cuenca, *Eur. J. Inorg. Chem.*, 2008, 4638.
20 J. Liimatainen, A. Lehtonen and R. Sillanpää, *Polyhedron*, 2000, **19**, 1133.
21 K. Most, J. Hoßbach, D. Vidović, J. Magull and N. C. Mösch-Zanetti, *Adv. Synth. Catal.*, 2005, **347**, 463; K. Heinze and A. Fischer, *Eur. J. Inorg. Chem.*, 2007, 1020; K. Hüttinger, C. Förster, T. Bund, D. Hinderberger and K. Heinze, *Inorg. Chem.*, 2012, **51**, 4180.
22 B. L. Tran and C. J. Carrano, *Inorg. Chem.*, 2007, **46**, 5429; A. J. Millar, C. J. Doonan, P. D. Smith, V. N. Nemykin, P. Basu and C. G. Young, *Chemistry*, 2005, **11**, 3255; V. N. Nemykin and P. Basu, *Inorg. Chem.*, 2005, **44**, 7494.
23 W. R. Thiel and T. Priermeier, *Angew. Chem., Int. Ed. Engl.*, 1995, **34**, 1737; J.-Y. Piquemal, S. Halut and J.-M. Brégeault, *Angew. Chem., Int. Ed.*, 1998, **37**, 1146; M. Herbert, F. Montilla, E. Álvarez and A. Galindo, *Dalton Trans.*, 2012, **41**, 6942; M. Bagherzadeh, M. Zare, V. Amani, A. Ellern and L. Keith Woo, *Polyhedron*, 2013, **53**, 223.
24 J. A. Brito, M. Gomez, G. Muller, H. Teruel, J.-C. Clinet, E. Dußach and M. A. Maestro, *Eur. J. Inorg. Chem.*, 2004, 4278.
25 J. Leppin, C. Förster and K. Heinze, *Inorg. Chem.*, 2014, **53**, 1039.
26 K. F. Morris and C. S. Johnson, *J. Am. Chem. Soc.*, 1993, **115**, 4291.

This journal is © The Royal Society of Chemistry 2015